Progress in Reaction Kinetics and Mechanism

ARTICLE

Open Access

https://doi.org/10.48130/prkm-0026-0009

Progress in Reaction Kinetics and Mechanism **2026**, 51: e018

Preparation of organophosphorus-rich tar and analysis of phosphorus-containing compounds in its pyrolysis products

Peiqi Chen[1], Guantao Shi[2], Nai Wang[2], Haining Tian[2], Yichen Zhang[1], Gang Li[1], Bin Su[3], Xiang Han[1], Anning Zhou[1], Qiuhong Wang[3], Zhenmin Luo[3] and Fuxin Chen[1*]

[1] *College of Chemistry and Chemical Engineering, Xi'an University of Science and Technology, Xi'an 710054, China*
[2] *Changqing Industrial Group Co., Ltd., Xi'an 710016, China*
[3] *College of Safety and Engineering, Xi'an University of Science and Technology, Xi'an 710054, China*
* Correspondence: chenfuxin1981@163.com (Chen F)

Abstract

This study utilized oil-rich coal as a material to achieve the effective preparation of organophosphorus-rich tar with enhanced value through co-pyrolysis in combination with different phosphorus-bearing substances. Through a comprehensive analysis of its chemical composition, the organic phosphine compounds were systematically studied and classified. Possible reaction pathways were proposed, laying a solid experimental foundation for the high-value conversion and application of coal tar. The molecular architecture and constituent profiles of valuable compounds within organophosphorus-rich tar were primarily analyzed using nuclear magnetic resonance (NMR) and gas chromatography coupled with mass spectrometry (GC-MS). Various phosphorus-containing reagents were introduced to explore the range of structures and types of organophosphorus species generated during co-pyrolysis. Under co-pyrolysis conversion conditions, various phosphorus sources are reacted with oil-rich coal to construct carbon-phosphorus (C-P) bonded molecules via a free radical-mediated chain reaction mechanism. This study establishes a green and efficient route to the high-value utilization of oil-rich coal, and a novel strategy for constructing C-P bonds was proposed.

Citation: Chen P, Shi G, Wang N, Tian H, Zhang Y, et al. 2026. Preparation of organophosphorus-rich tar and analysis of phosphorus-containing compounds in its pyrolysis products. *Progress in Reaction Kinetics and Mechanism* 51: e018 https://doi.org/10.48130/prkm-0026-0009

Introduction

China's energy profile, characterized by 'limited oil reserves, scarce natural gas resources, and relatively abundant coal reserves', drives innovation in the field of coal-based energy and chemical engineering[1]. Beyond its role as a principal energy carrier, coal serves as an essential raw material for generating synthetic liquid fuels, combustible gases, and valuable chemical substances with high economic returns[2]. Among these, oil-rich coal shows considerable promise for utilization due to its superior ability to produce increased quantities of oil and gas during thermal decomposition processes[3]. Functional groups act as essential structural units in molecular frameworks. The chemical composition of oil-rich coal is marked by a high hydrogen content and the presence of thermally labile, weak chemical bonds. These characteristics promote the efficient formation and concentration of liquid tar during pyrolysis and related thermochemical conversion processes, thus offering a distinct advantage as a feedstock for the selective synthesis of high-value-added chemical substances[4]. Therefore, conducting systematic research on the identification of oil and gas resource attributes in oil-rich coal and exploring pathways for its green and low-carbon development hold significant theoretical value and practical guidance for advancing the clean and efficient conversion of coal resources[5].

The resource potential of oil-rich coal can be realized through targeted conversion technologies, enabling the selective synthesis of high-value-added chemical products[6]. Pyrolysis technology constitutes a fundamental and pivotal step in enabling the directional conversion of coal. Thermochemical treatment decomposes complex coal macromolecules into liquid tar, syngas, and solid semi-coke. The differentiated utilization of these three-phase products exemplifies the hierarchical transformation and cascaded utilization of coal resources, thereby establishing fundamental pathways for resource-efficient and value-added utilization[7]. The tar obtained from the pyrolysis of oil-rich coal is highly enriched in aromatic hydrocarbons, phenolic compounds, and heterocyclic species, which possess considerable application potential in the synthesis of aviation fuels[8], photovoltaic materials[9], and pharmaceutical intermediates[10]. However, current pyrolysis technologies face dual challenges of low tar yields and excessively high concentrations of heavy components, which not only limit the overall operational efficiency of processing systems but also significantly hinder the downstream upgrading and utilization of derived oil products[11]. Consequently, the development of novel pyrolysis technologies capable of precisely controlling reaction processes to achieve simultaneous improvements in both hydrocarbon quality and yield constitutes a key research direction in this field[12]. Recent studies have shown that rational modulation of the feedstock composition during coal co-pyrolysis can effectively optimize reaction pathways, thereby promoting the efficient resource utilization of coal. The primary technical strategies include co-pyrolysis with biomass[13–15], catalytic pyrolysis[16–18], and hydropyrolysis[19–22].

Phosphorus is widely distributed in the Earth's crust and plays a vital role in metabolic activities and the construction of structural components in living organisms[23]. Organophosphorus compounds exhibit essential functional properties across diverse fields such as pharmaceuticals, agriculture, and materials science. Their applications range from the conventional production of phosphorus fertilizers and pesticides[24] to the modern development of flame retardants and plasticizers[25,26], and further extend to the functional design of bioactive molecules and advanced materials[27]. The underlying molecular architecture critically depends on the precise

formation of carbon-phosphorus bonds, which has become a central focus in contemporary research. Current methodologies primarily rely on nucleophilic or electrophilic phosphonylation pathways[28,29], which suffer from limited reaction diversity, poor functional group tolerance, and frequent requirements for stringent anhydrous and anaerobic conditions. These limitations have emerged as a major bottleneck hindering the scalable synthesis of organophosphorus functional molecules[30]. Moreover, heteroatom doping has been widely recognized as an effective strategy for the functional modification of biomass-derived carbon materials. By introducing heteroatoms into the carbon lattice, this approach significantly improves material performance and expands its application potential[31]. Chen et al.[32] successfully synthesized nitrogen-enriched tar through the co-pyrolysis of ammonium chloride and oil-rich coal. Yi et al.[33] fabricated phosphorus-doped hierarchically porous carbon microspheres (A-PCM) via a hydrothermal method. The resulting material exhibits excellent electrical conductivity and can function as a high-performance electrocatalyst in oxidase-mimicking sensors and supercapacitors. However, research on organophosphorus-rich tar remains scarcely reported. To bridge this knowledge gap, the present study investigates the co-pyrolysis of oil-rich coal with various phosphorus-containing compounds. The complex aromatic architecture of coal provides a diverse array of carbon precursors conducive to carbon-phosphorus (C-P) bond formation, while the abundant free radicals generated during pyrolysis offer an efficient pathway for direct and rapid C-P bond construction. Through *in situ* free radical chain reactions, organophosphorus-rich tar compounds are successfully prepared, thereby establishing a green and highly efficient route for the valorization of oil-rich coal.

Currently, the chemical analysis of coal tar predominantly relies on gas chromatography (GC) and its hyphenated analytical techniques[34]. Among these, gas chromatography-mass spectrometry (GC-MS) integrates the high separation efficiency of chromatography with the qualitative capabilities of mass spectrometry, enabling rapid screening of multicomponent mixtures in a relatively short time[35]. El-Saeid et al.[36] employed the GC-MS-TIC technique for the determination of organophosphorus components among 220 pesticides. However, this method exhibits limited responsiveness to high-boiling-point phosphorus compounds that are difficult to vaporize. Furthermore, the presence of abundant coexisting hydrocarbons in coal tar suppresses the sensitivity of phosphorus signal detection, resulting in the omission of certain target analytes. To address these limitations, gas chromatography-flame photometric detection (GC-FPD) has emerged as the method of choice for the preliminary screening of phosphorus-containing compounds in complex matrices, owing to its high selectivity and sensitivity toward phosphorus. A single injection enables the simultaneous identification of multiple phosphorus-containing components[37]. Wiktorko et al.[38] conducted a comparative evaluation of the ultra-sensitive detection capabilities of GC-FPD and GC-ICP-MS for organophosphorus compounds. However, flame photometric detection (FPD) provides only retention time data and cannot directly elucidate molecular structures, necessitating extensive comparisons with standard compounds associated with high workload and prolonged analysis time. To overcome the limitations of chromatographic methods in structural identification, nuclear magnetic resonance spectroscopy (NMR) can be employed as a complementary analytical technique. Phosphorus-31 (^{31}P) has a natural abundance of 100% and exhibits high sensitivity in nuclear magnetic resonance (NMR) detection. Two-dimensional NMR (2D NMR) techniques have been widely used to elucidate the structures of complex organic molecules and biomacromolecules, as well as to investigate intermolecular interactions, thereby effectively reducing spectral overlap[39]. In particular, two-dimensional hydrogen-phosphorus correlation spectroscopy (^{1}H-^{31}P 2D NMR) enables unambiguous assignment of directly bonded H-P correlations within a short experimental time, significantly decreasing both measurement duration and sample consumption. This method serves as a robust complementary tool for the rapid structural characterization of phosphorus-containing compounds. Ma et al.[40] employed conventional ^{1}H-^{31}P HMBC spectroscopy to analyze glycerol phospholipids and identified characteristic chemical shifts in the ^{1}H-^{31}P HMBC spectra, thereby demonstrating its utility in characterizing phospholipid profiles across 18 marine algal species.

Based on the aforementioned experimental studies, this research utilized Zhangjiamao oil-rich coal as the raw material for co-pyrolysis with various phosphorus-containing compounds, leading to the successful preparation of organophosphorus-rich tar. Given the complexity and structural diversity of organophosphorus in the tar, a systematic analytical approach was employed. First, phosphorus content variations were quantified using ICP-OES. Subsequently, the coal tar was analyzed by gas chromatography-flame photometric detection (GC-FPD) and gas chromatography-mass spectrometry (GC-MS), enabling structural characterization of organophosphorus species based on mass spectral data. Finally, the molecular speciation of organic phosphorus in the resulting products was further confirmed through ^{31}P NMR and ^{1}H-^{31}P heteronuclear multiple-bond correlation (HMBC) NMR techniques.

Materials and methods

Materials

The rich-oil coal used in this article is from the Zhangjiamao area in Shenmu City, Yulin City, Shaanxi Province, China. It mainly exists in the 5-2 coal seam of the Yan'an Formation of the Jurassic System. The samples were subsequently crushed and sieved to achieve a particle size of less than 200 mesh. The proximate analysis was performed in accordance with GB/T 212-2008 'Proximate Analysis of Coal', and the elemental composition was determined using an Elementar Vario EL III elemental analyzer; the results are presented in Table 1. The Zhangjiamao coal sample is classified as a medium to low-rank coal with a high H/C atomic ratio, indicative of substantial hydrogen abundance, which facilitates the release of abundant active hydrogen radicals during the initial pyrolysis stage. This provides a sufficient in situ hydrogen source for the reduction of compounds containing P=O bonds. Moreover, the coal is rich in aromatic and aliphatic fragments, thereby serving as a robust feedstock for the synthesis of high-value chemicals and organophosphorus-rich tars. All experimental reagents were obtained from Shanghai Macklin Biochemical Technology Co., Ltd., and had a purity of 99%.

Table 1. Industrial analysis and elemental analysis of oil-rich coal samples.

Sample	Industrial analysis (%)				Elemental analysis (%)					
	M_{ad}	A_{ad}	V_{ad}	FC_{ad}	C	H	O	N	S	H/C
Coal of Zhangjiamao	3.78	6.92	32.51	56.79	77.89	4.62	16.51	0.60	0.38	0.71

Co-pyrolysis experiment

All the co-pyrolysis experiments conducted in this paper were carried out in a custom-built thermal decomposition furnace. Prior to the experiment, 0.2 g of oil-rich coal and 0.2 g of a phosphorus-containing compound were thoroughly mixed and sealed in a stainless-steel tube (70 mm in length, 5 mm outer diameter, 4 mm inner diameter). The sealed tube was then placed into a quartz tube reactor (10 mm outer diameter, 400 mm effective length), and secured at both ends with quartz wool plugs. Subsequently, the assembly was inserted into the pyrolysis reactor, connected to the experimental apparatus, and the temperature ramp program was initiated. During the experimental procedure, nitrogen gas was continuously introduced at a flow rate of 20 mL/min for a pyrolysis duration of 10 min. Throughout the pyrolysis process, the resultant products gradually migrated downward through the quartz tube. Due to the sharp temperature gradient in the lower section of the tube, the tar components preferentially condensed into the liquid phase. The uncondensed fractions were subsequently trapped by acetone placed at the bottom of the system. After completion of the pyrolysis experiment, the solvent was completely evaporated under controlled conditions, and the collected coal tar was accurately weighed for subsequent characterization and analysis.

Determination of phosphorus content by ICP-OES analysis

Given that coal tar constitutes a complex organic matrix, the complete release and detection of its phosphorus content requires thorough prior digestion of the organic constituents. Microwave digestion technology, known for its high efficiency and safety, enables the processing of complex organic samples by achieving complete matrix decomposition and ensuring quantitative dissolution of target elements within a short period. This study employed microwave digestion for the pretreatment of coal tar samples and used an Agilent 5110 inductively coupled plasma optical emission spectrometer (ICP-OES) to accurately determine the phosphorus content in the tar.

FTIR analysis

Structural and functional group analyses of coal tar derivatives were performed using a Thermo Scientific FTIR spectrometer under the following conditions: 2-min scan duration, a spectral resolution of 0.4 cm^{-1}, and a wavenumber range of 400–4,000 cm^{-1}. Sample preparation was carried out using the potassium bromide (KBr) pellet method, with a coal tar-to-KBr mass ratio of 1:200. The mixture was thoroughly ground and homogenized prior to compression into pellets using a hydraulic press. Data interpretation was conducted using the OMNIC software suite.

GC-FPD analysis

GC-FPD exhibits high selectivity and exceptional sensitivity for the analysis of phosphorus-containing compounds. This technique offers reliable and highly sensitive detection of phosphorus species, with outstanding selectivity under optimized conditions. The experiment employed an 8890 gas chromatograph-FPD detector (Shimadzu Corporation, Japan), and an HP-5MS capillary column. The temperature program was as follows: initial temperature held at 60 °C for 1 min, increased to 150 °C at a rate of 10 °C/min (held for 0 min), then ramped to 310 °C at 4 °C/min with a final hold time of 10 min. The split ratio was maintained at 10:1, and the vaporization chamber temperature was set at 290 °C. The carrier gas (nitrogen) flow rate was kept constant at 1.0 mL/min, with hydrogen and air flow rates set at 30 and 300 mL/min, respectively. The FPD detector temperature was maintained at 320 °C, and the makeup gas flow rate was 30 mL/min. Under the optimized temperature programming conditions, baseline separation of organophosphorus compounds was achieved on the HP-5MS column, along with a strong signal response in the FPD.

GC-MS analysis

The coal tar obtained from the experiment was diluted with acetone to a concentration of 1 mg/mL, and the split ratio of GC-MS was 50:1. The initial temperature of 80 °C was held for 1 min, followed by a ramp at 20 °C/min to 310 °C, which was maintained for 4 min. Pyrolysis products were identified by gas chromatography-mass spectrometry (GC-MS) with reference to the NIST 14 mass spectral library. Each sample was analyzed in replicate to ensure data reproducibility and reliability.

Nuclear magnetic resonance (NMR) analysis

The nuclear magnetic resonance instrument used in this article is of model 400MHz Bruker Avance III HD. This instrument is equipped with a PA BBO 400S1 BBF-H-D-05 Z SP probe. The experimental temperature was maintained at 298 K. Fifty mg of tar was taken, and 500 μL of DMSO was added to dissolve it completely, which was then loaded into the NMR tube. The ^{31}P NMR used the zgpg30 pulse sequence with NS = 16, and DS = 4; the ^{1}H-^{31}P HMBC used the HMBCGPNDQF pulse sequence with NS = 8, and DS = 16. All spectra were analyzed and processed using the Bruker Topspin 4.1.1 software.

Results and discussion

The study initially investigated the tar yields obtained from the co-pyrolysis of phosphorus-containing compounds with oil-rich coal under varying temperatures. The results show that tar coloration intensifies with increasing temperature, although this chromatic change becomes less pronounced above 600 °C. Building on previous research, it was found that excessively low temperatures resulted in incomplete reactions, whereas excessively high temperatures promoted a greater number of side reactions. In contrast, 600 °C was identified as the optimal reaction temperature. Furthermore, the reactant ratio during the pyrolysis process is of critical importance. This study investigates the effects of varying the ratio of oil-rich coal to phosphorus-containing compound at 1:1, 1:3, and 1:5, as shown in Fig. 1. The findings reveal that as the proportion of phosphorus-containing compounds gradually increases, the composition of phosphorus-containing species across the three tar groups exhibits a high degree of consistency, indicating that, under the experimental conditions investigated, a 1:1 ratio represents the optimal condition. Regarding the reaction duration, it was found that a too short reaction duration would result in incomplete reaction, while a too long reaction duration would cause the tar to undergo secondary cracking. Therefore, the reaction duration is set at 2 min.

Modification of coal pyrolysis through inorganic phosphorus source doping

Common inorganic phosphorus sources primarily include phosphoric acid and its salt derivatives, such as H_3PO_4, KH_2PO_4, and $NH_4H_2PO_4$. This study selects the aforementioned phosphorus

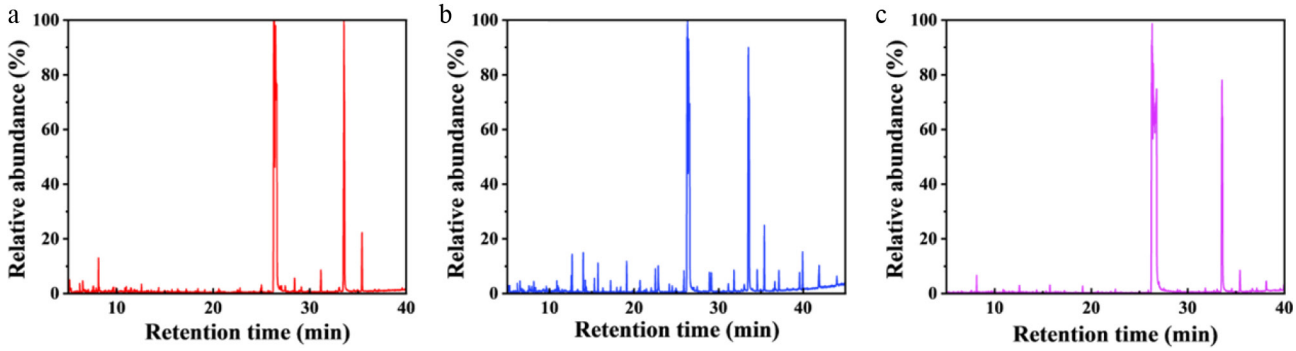

Fig. 1 The TIC diagrams of the tar obtained by the co-pyrolysis of rich-oil coal and phosphorus-containing compounds at different ratios. Ratio is all rich-oil coal : phosphorus compounds, (a) 1:1, (b) 1:3, (c) 1:5.

sources to conduct co-pyrolysis experiments with oil-rich coal, aiming to investigate the transformation behavior of phosphorus during pyrolysis and its influence on the distribution of pyrolysis products. Analysis based on GC-MS detection results indicates a limited presence of target-effective phosphine compounds. This phenomenon can be attributed to the ability of the phosphorus atom, possessing accessible 3d orbitals, to engage in back-bonding interactions with lone pair electrons located in the 2p orbitals of oxygen atoms, thereby increasing P-O bond energy. Additionally, the tetrahedral phosphate unit exhibits high symmetry, which facilitates the formation of a delocalized π-system and further enhances bond stability. The negative charge of the phosphate ion is evenly distributed across the four oxygen atoms, minimizing electron-electron repulsion on any individual oxygen center. Concurrently, the P(V) oxidation state reduces bond polarity and increases the covalent character of the P-O bonds, both factors favoring π-bonding interactions and contributing to elevated bond strength. However, it is noteworthy that despite the high bond energy of P-O bonds, a small fraction of these bonds undergoes cleavage under pyrolysis temperature conditions, generating phosphorolyoxy radicals that can be stabilized through resonance involving the 3d orbitals of the phosphorus atom. In contrast, hydroxyl radicals produced by O-H bond cleavage do not exhibit significant stabilization. Consequently, a minor proportion of the P-O bonds ruptures at elevated temperatures and subsequently reacts with phenolic compounds released during coal pyrolysis. However, in phenol, the pronounced polarity of the O-H bond, combined with the high electronegativity of the oxygen atom and p-π conjugation with the benzene ring, results in reduced electron cloud density on the oxygen atom and a consequent weakening of the O-H bond, thereby facilitating the formation of monophenyl phosphate, as shown in Fig. 2.

Secondly, among the halogenated phosphorus compounds, PBr_3 and PCl_3 are the most representative. Theoretically, cleavage of the P-X bonds in these compounds can generate multiple active sites, thereby providing abundant reactive positions for subsequent phosphorylation reactions. However, GC-MS and NMR analyses revealed that both systems generated limited quantities of effective organophosphorus compounds. Notably, weak signals were still detected in the ^{31}P NMR spectrum of the PBr_3 co-pyrolysis with oil-rich coal. To assign these signals, reference ^{31}P NMR chemical shifts of various phosphorus standards were acquired in advance and compiled in Table 2. Comparative analysis indicated that the co-pyrolysis products from PBr_3 and coal predominantly consisted of phosphoric acid along with minor amounts of dialkyl phosphates, whereas those from PCl_3 and oil-rich coal were primarily phosphoric acid. This discrepancy can be attributed to the low boiling point of PCl_3 (76 °C), which leads to its volatilization before the coal matrix reaches the intense thermal cracking stage, enabling a substantial portion of PCl_3 to escape the reaction zone as vapor, and subsequently react with atmospheric oxygen and moisture to form phosphoric acid.

Both phosphorus halides in the P(III) and P(V) oxidation states exhibit the aforementioned limitations. Therefore, this study employs $POCl_3$ for co-pyrolysis with oil-rich coal, owing to its favorable characteristics: it not only contains relatively reactive P-Cl bonds but also features phosphorus atoms in the P(V) oxidation state, which

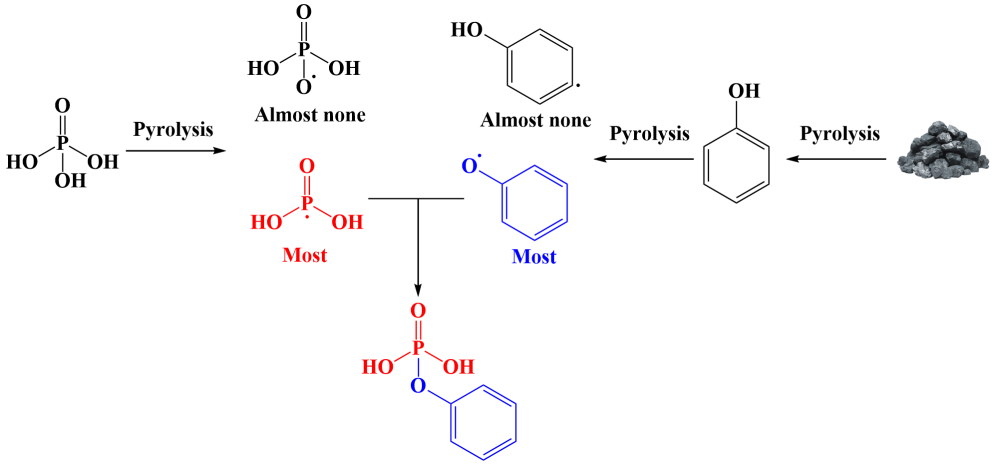

Fig. 2 Speculation on the mechanism of the co-pyrolysis products of phosphoric acid and coal.

Table 2. ^{31}P NMR chemical shifts of phosphorus-containing standards.

No.	Compound name	Solvent	δ_P (ppm)
1	Triphenyl phosphite	$CDCl_3$	128.5
2	Methyl diphenylphosphinite	$CDCl_3$	116.92
3	Chlorodiphenylphosphine	$CDCl_3$	81.88
4	Diphenylphosphinic chloride	$CDCl_3$	44.68
5	Dichlorophenylphosphine	$CDCl_3$	36.02
6	Phenylphosphonic dichloride	$CDCl_3$	35.98
7	Methyldiphenylphosphine oxide	$CDCl_3$	29.90
8	Phenylphosphonic acid dimethyl ester	$CDCl_3$	27.04
9	Phosphate radical (Na_3PO_4)	$CDCl_3$	6
10	Phosphoric acid	$CDCl_3$	0
11	Triphenylphosphine	$CDCl_3$	−5.38
12	(±) 2,2'-bis(diphenylphosphino)-1,1'-binaphthyl	C_6D_6	−15.61
13	Triethylphosphine	$CDCl_3$	−20
14	Methyl(diphenyl)phosphane	$CDCl_3$	−26.7
15	Tri(1-naphthyl)phosphine	D_6-DMSO	−33.14
16	Dimethylphenylphosphine	$CDCl_3$	−45.46
17	Trimethylphosphine	$CDCl_3$	−62
18	Phosphorus pentachloride	$CDCl_3$	−80

prevents further oxidation. Figure 3a presents the total ion current (TIC) chromatogram of the co-pyrolysis products from phosphorus oxychloride and oil-rich coal. A peak-by-peak analysis of all signals in the TIC chromatogram, performed using the NIST 14 mass spectral library, revealed that the tar products contained only two detectable organophosphorus compounds. Due to the inherent uncertainty associated with spectral library comparisons, the phosphorus content in the raw coal pyrolysis tar and in the co-pyrolysis coal tar was compared using ICP-OES analysis. Table 3 indicates that the introduction of phosphorus-containing compounds during co-pyrolysis results in an approximately 500-fold increase in the phosphorus content of the derived tar compared to the phosphorus-free condition. The mass fraction calculated from GC-MS peak areas shows a discrepancy relative to the results obtained by ICP-OES analysis. Subsequent GC-FPD analysis of the co-pyrolysis tar demonstrated that this detector provides detection sensitivity for phosphorus-containing compounds at the μg/L level. As illustrated in Fig. 3b, the co-pyrolysis products contain at least 22 phosphorus-containing compounds, indicating that GC-MS analysis faces inherent limitations for such species. This limitation can be attributed to the generation of numerous high-molecular-weight aromatic and aliphatic compounds during coal pyrolysis. These compounds may react with phosphorus-containing species to form large-molecular-weight organophosphorus derivatives, which typically exhibit high boiling points and low vapor pressures. Consequently, the concentration of these molecules per unit volume is insufficient to reach the detection limit, even if they enter the ionization source. However,

Table 3. Comparison of P content in raw coal pyrolysis tar and co-pyrolysis coal tar.

Sample name	Treatment method	Content of P (mg/L)
Coal pyrolysis tar	Microwave digestion	1.04
Phosphorus-containing co-pyrolysis tar	Microwave digestion	546.84

structural elucidation of the target compounds by GC-FPD analysis remains challenging. The FPD detector provides only one-dimensional retention time data, necessitating laborious and time-consuming assignment of phosphorus-containing functional groups through comparison of each chromatographic signal with corresponding reference standards. Consequently, auxiliary analytical techniques are indispensable for determining the precise structures of specific phosphine compounds present in the tar.

Figure 4 presents the ^{31}P NMR spectrum of the co-pyrolysis products from phosphorus oxychloride and oil-rich coal. The spectrum reveals the presence of more than two types of organophosphorus compounds, further corroborating certain limitations in the GC-MS analysis of phosphorus-containing species. The NMR spectrum was divided into three regions. Based on the reference spectra of standard phosphorus-containing compounds provided in Table 1, it was inferred that the signals in the 15–35 ppm region primarily originate from alkyl phenylphosphine oxides formed through cleavage of the P-Cl bonds in phosphorus oxychloride and subsequent reactions with aryl or aliphatic radicals generated during coal pyrolysis. As the chemical shift decreases, this indicates a gradual reduction in the electron density around the phosphorus atom. For the P=O bond, due to the negative hyperconjugation between the O atom and the P atom, that is, there is a feedback bond between them, the electrons in the 3d orbital of the P atom shift to the 2p orbital of the O atom, resulting in a decrease in electron density and a relatively high chemical shift. Consequently, within the chemical shift range of −5 to 5 ppm, signals corresponding to phosphoric acid, phenyl phosphate, and related compounds are predominantly observed. The dual activation of phosphorus-arising from the presence of highly coordinated vacant d-orbitals and the strong electron-withdrawing effect of the P=O bond on the phosphorus atom-renders the P-Cl bond highly susceptible to nucleophilic attack by water molecules, leading to the formation of phosphoric acid. Meanwhile, phenyl phosphate is generated through the coupling of phosphoric acid intermediates with phenolic radicals released from coal during the acid-formation process. Secondly, the emergence of phosphorus (III) phosphine compounds within this region indicates partial reduction of P=O bonds. Given the overall pyrolysis conditions, it is hypothesized that coal decomposition releases a substantial quantity of hydrogen radicals during thermal degradation, which possess reducibility and contribute to this reduction process. The reduction

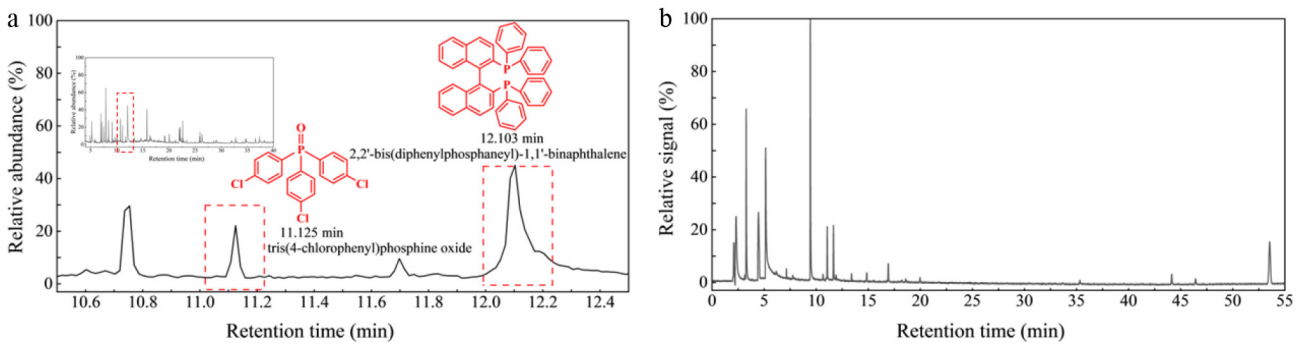

Fig. 3 GC diagram of the co-pyrolysis products of $POCl_3$ and oil-rich coal. (a) GC-MS; (b) GC-FPD.

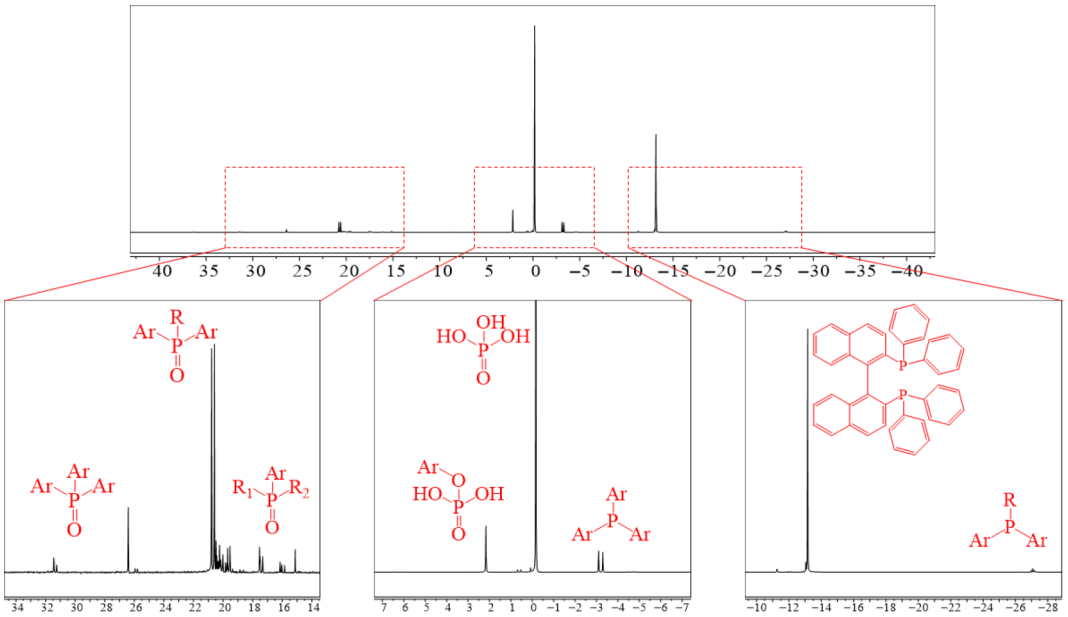

Fig. 4 ^{31}P NMR images of the co-pyrolysis products of phosphorus oxychloride and oil-rich coal, and the structures of phosphine compounds in various regions.

of P=O bonds is followed by reactions with aryl and alkyl groups generated from coal pyrolysis to form alkylphenyl phosphine oxides, a feature also reflected in the chemical shift range of −30 to −10 ppm. However, based on the chemical shifts of reference compounds, it can be inferred that the content of triarylphosphines far exceeds that of diarylalkylphosphines, while dialkylarylphosphines and trialkylphosphines are virtually undetectable. This phenomenon is likely attributable to the three aromatic rings facilitating delocalization of the electron density around the phosphorus atom through π-π conjugation, while simultaneously forming a sterically hindered cage-like structure that reduces the likelihood of interaction between the phosphorus center and oxygen, water, or other reactive radicals. This interpretation is supported by the observed chemical shifts of multi-alkyl-substituted phosphine oxides (approximately 20 ppm), and multi-aryl-substituted phosphine oxides (approximately -3 ppm).

Concurrently, this study performed infrared spectroscopy analysis on the tar. Identification of key absorption peaks revealed a stretching vibration band attributable to P=O at 1,257 cm^{-1}, corresponding to the backbone structure of newly formed phosphine oxide compounds generated during the pyrolysis of phosphorus oxychloride. Additionally, a C-P stretching vibration band was observed at 1,008.4 cm^{-1}, indicating successful formation of the carbon-phosphorus bond in the reaction, which serves as critical evidence for the generation of organophosphorus compounds. Notably, a weak absorption peak was detected at 1,085 cm^{-1} and assigned to the P-O-C linkage, suggesting the formation of phosphonate esters during the reaction process. This observation is consistent with the presence of aromatic phosphonate esters detected near δ = 2 ppm in Fig. 4. Furthermore, all identified infrared absorption bands show strong consistency with the results from GC-MS and NMR analyses.

Incorporation of organophosphorus compounds and coal pyrolysis

Initially, co-pyrolysis experiments were carried out using oil-rich coal and phosphonate compounds as the phosphorus source. Similar to phosphates, phosphonates also contain P-O bonds in their molecular backbone. However, a key distinction is that the alkoxy or aryloxy substituents in phosphonates exert electron-donating effects, which increase the electron density around the phosphorus atom and thereby weaken the attractive interaction between phosphorus and oxygen. Consequently, the bond dissociation energy of the P-O bond is reduced, leading to a higher yield of decomposition products from organic phosphonates under identical pyrolysis conditions. Co-pyrolysis of oil-rich coal with dimethyl phenylphosphonate was conducted, and Fig. 5a presents the ^{31}P NMR spectrum of the resulting co-pyrolysis products. The signals are predominantly distributed in the 0–50 ppm region. According to the data in Table 2, this region is primarily assigned to compounds containing P=O functional groups. Based on the ^{31}P NMR analysis, it is preliminarily inferred that these signals likely originate from aryl- and alkyl-substituted phosphine oxides. However, further structural characterization of these compounds cannot be achieved based solely on the ^{31}P NMR data.

The ^{1}H-^{31}P HMBC technique enables rapid screening of target compound coupling information in complex matrices. The co-pyrolysis tar was subjected to ^{1}H-^{31}P HMBC analysis, with the results presented in Fig. 5b. As illustrated, the P coupling signals predominantly appear within the 20–40 ppm range, whereas the H coupling signals exhibit a broad distribution. This observation supports the preliminary conclusion drawn previously. Figure 5c illustrates the co-pyrolysis mechanism of diphenyl methylphosphonate and oil-rich coal. Integration with the ^{1}H-^{31}P HMBC NMR spectrum reveals that at δ_P = 20 ppm, four distinct hydrogen coupling signals are observed in the low-field region, indicating the presence of at least two different aromatic groups bonded to the phosphorus atom. However, a coupling signal is observed at δ_H = 3.7 ppm. Based on the characteristic chemical shifts of functional groups, alkyl groups are first ruled out since typical alkyl protons exhibit chemical shifts around δ_H = 1–2 ppm. Alkoxy groups are subsequently excluded as well; although alkoxy protons generally resonate near δ_H = 3.5 ppm, HMBC relies on long-range J-coupling for signal transmission. Given the high electronegativity of oxygen, which draws electron density from adjacent bonds, the corresponding two-bond (^{2}J), or

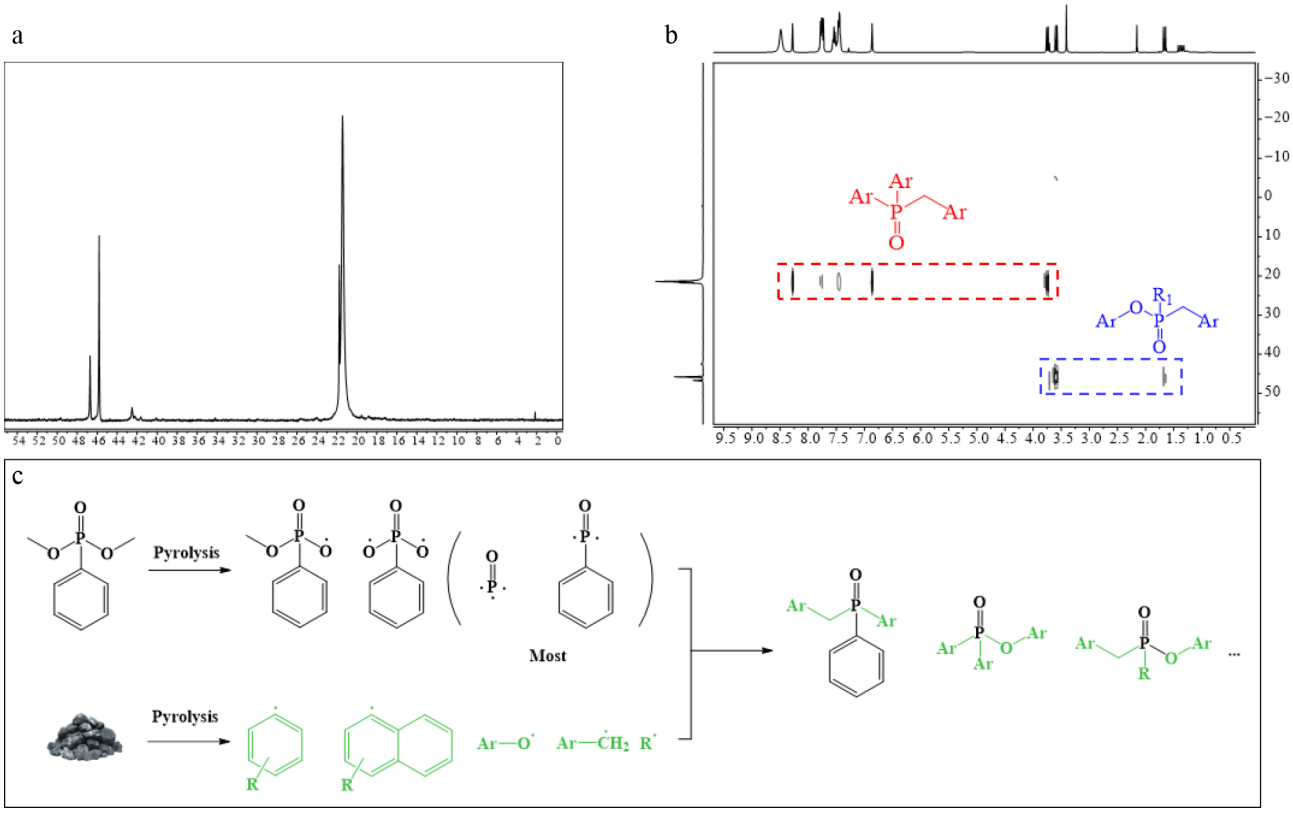

Fig. 5 NMR spectra and mechanism diagrams of the co-pyrolysis products of dimethyl phenylphosphonate and oil-rich coal. (a) ^{31}P NMR spectrum; (b) ^{1}H-^{31}P HMBC NMR spectrum; (c) mechanism diagram.

three-bond (^{3}J) coupling constants approach 0 Hz. As a result, no ^{1}H-^{31}P coupling signal is detected under these conditions. The δ_H chemical shift observed for the benzylic proton at 2.5–3 ppm, although outside the typical aromatic region, can be rationalized by the electron-withdrawing effect of the adjacent phosphine oxide group (P=O), which induces a downfield shift. This interpretation is consistent with the observed ^{1}H-^{31}P HMBC correlation signal, thereby confirming the structural assignment as a diaryl benzylphosphine oxide. In addition, coupled signals are partially observed at approximately δ_P = 40 ppm; however, these signals do not appear in the downfield region. This observation suggests two possibilities: either the compound lacks an aromatic ring system, or its ^{1}H-^{31}P correlations are shielded by oxygen atoms. Based on the phosphorus chemical shift, which is only slightly higher than that of the previously analyzed diaryl benzylphosphine oxide, it can be inferred that the two structures are closely related. Therefore, the absence of detectable ^{1}H-^{31}P signals is likely attributable to oxygen-induced shielding. The high electronegativity of oxygen reduces the electron density around the P=O bond, resulting in a marginally upfield-shifted resonance. Similarly, the coupling signal at δ_H = 3.7 ppm originates from the benzyl group, while the signal at δ_H = 1.6 ppm arises from an alkyl group. Therefore, the molecular structure associated with this phosphorus center can be assigned as phenyl benzylalkylphosphonate.

Secondly, co-pyrolysis experiments were conducted between oil-rich coal and triphenyl phosphite (which lacks P=O functional groups). The resulting ^{31}P NMR spectrum of the products is presented in Fig. 6. However, no cross-peaks were detected in the corresponding ^{1}H-^{31}P HMBC analysis. According to previous research findings, triphenyl phosphate exhibits a δ_P chemical shift of approximately -17 ppm[41], which aligns with one of the signals observed in

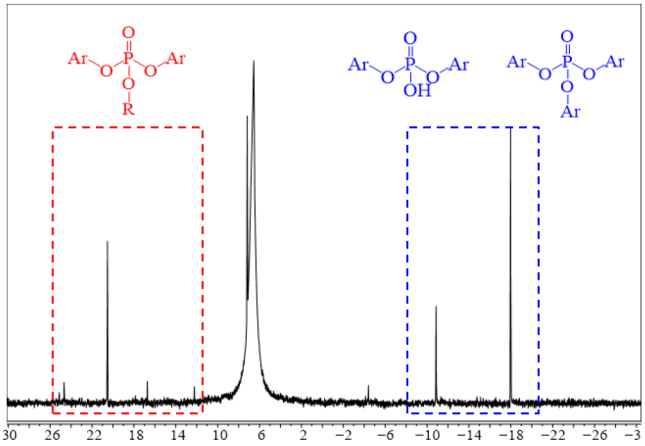

Fig. 6 The ^{31}P NMR spectrum of the co-pyrolysis products of triphenyl phosphite and oil-rich coal.

Fig. 6. The remaining signals were identified through comparison of substituents listed in Table 1 as diaryl phosphates and various alkyl-aryl substituted phosphates. The characteristic structural feature of these phosphates is the basic skeleton composed of one P=O bond and three P-O bonds, which is the key reason for the absence of signals in the ^{1}H-^{31}P HMBC spectrum. The formation of these phosphates can be attributed to the conjugation effect in triphenyl phosphite, which confers a substantially higher bond energy to the C-O bond compared to the P-O bond. Consequently, cleavage of these bonds releases a significant amount of phenol radicals. The resulting phosphorus radicals are highly susceptible to oxidation, converting into phosphate-type compounds, which subsequently combine

with phenol radicals or other phenolic radicals generated during coal pyrolysis to form triaryl phosphates and various aryl alkyl phosphonates.

Co-pyrolysis of oil-rich coal and non-phosphonate compounds

This study also conducted co-pyrolysis experiments with oil-rich coal and organophosphorus compounds lacking P=O functional groups. Similarly, pyrolysis was performed using dimethylphenylphosphine, which possesses mixed substituents, in combination with oil-rich coal. The results revealed a single signal in the ^{31}P NMR spectrum of the product, which was attributed to dimethylphenylphosphine oxide. This assignment is supported by the relatively low boiling point of dimethylphenylphosphine compared to other phosphine compounds. Under the experimental conditions employed, dimethylphenylphosphine volatilized in gaseous form prior to the cleavage of the C-P bond, and was subsequently oxidized in air to form dimethylphenylphosphine oxide. Subsequently, phenylphosphonic dichloride was employed, and the ^{31}P NMR spectrum of its product is depicted in Fig. 7a. The signals in the spectrum indicate that the product derived from phenylphosphonic dichloride is substantially more abundant than the previously obtained phosphorous-containing compounds, with the signals predominantly concentrated in the range of δ_P = 15–65 ppm. In addition, ^{1}H-^{31}P HMBC detection was conducted on them, as shown in Fig. 7b. It is speculated that these compounds are all derived from phosphonate aryl esters or phosphonate diaryl esters, and their reaction mechanisms are shown in Fig. 7c. This can be attributed to the relative lability of the P-Cl bond in phenyl dichlorophosphine, which readily undergoes cleavage, allowing the resulting P(III) species to be oxidized to P(V) and subsequently react with various aromatic and aliphatic radicals released from coal to form diverse phosphonate esters. Although conjugation between the P=O group and the phenyl ring enhances the stability of the P-C bond compared to the P-Cl bond, partial substitution of the phenyl group by aliphatic radicals derived from coal is evidenced by the isolated signal observed near δ_H = 1.2 ppm in Fig. 7b.

Similarly, chlorinated diphenylphosphine is co-pyrolyzed with coal. The difference between it and phenylphosphine dichlorophene lies in the number of phenyl and chlorine substituents, which makes it relatively easy for only one P-Cl to break. The reaction mechanism diagram is shown in Fig. 8c. Figure 8a and b presents the ^{31}P NMR spectrum and the ^{1}H-^{31}P HMBC NMR spectrum of this compound. Comparison with the ^{31}P NMR spectrum of phenyldichlorophosphine reveals a marked reduction in signal intensity for chlorodiphenylphosphine; however, the signals remain more abundant than those observed for previously studied phosphorus-containing compounds-again attributable to the facile cleavage of the P-Cl bond. As with phenyldichlorophosphine, all signals in the ^{31}P NMR spectrum appear within the δ_P = 20–50 ppm range, indicating a high degree of structural similarity among the phosphorus-containing products derived from both precursors. The ^{1}H-^{31}P HMBC NMR spectrum shows weakened correlations in both aromatic and aliphatic regions, with no distinct aliphatic cross-peaks detected. This suggests that the two phenyl groups in chlorodiphenylphosphine are less susceptible to elimination, thereby limiting its interaction with coal to chlorine substitution by aromatic and aliphatic radicals released from the coal matrix.

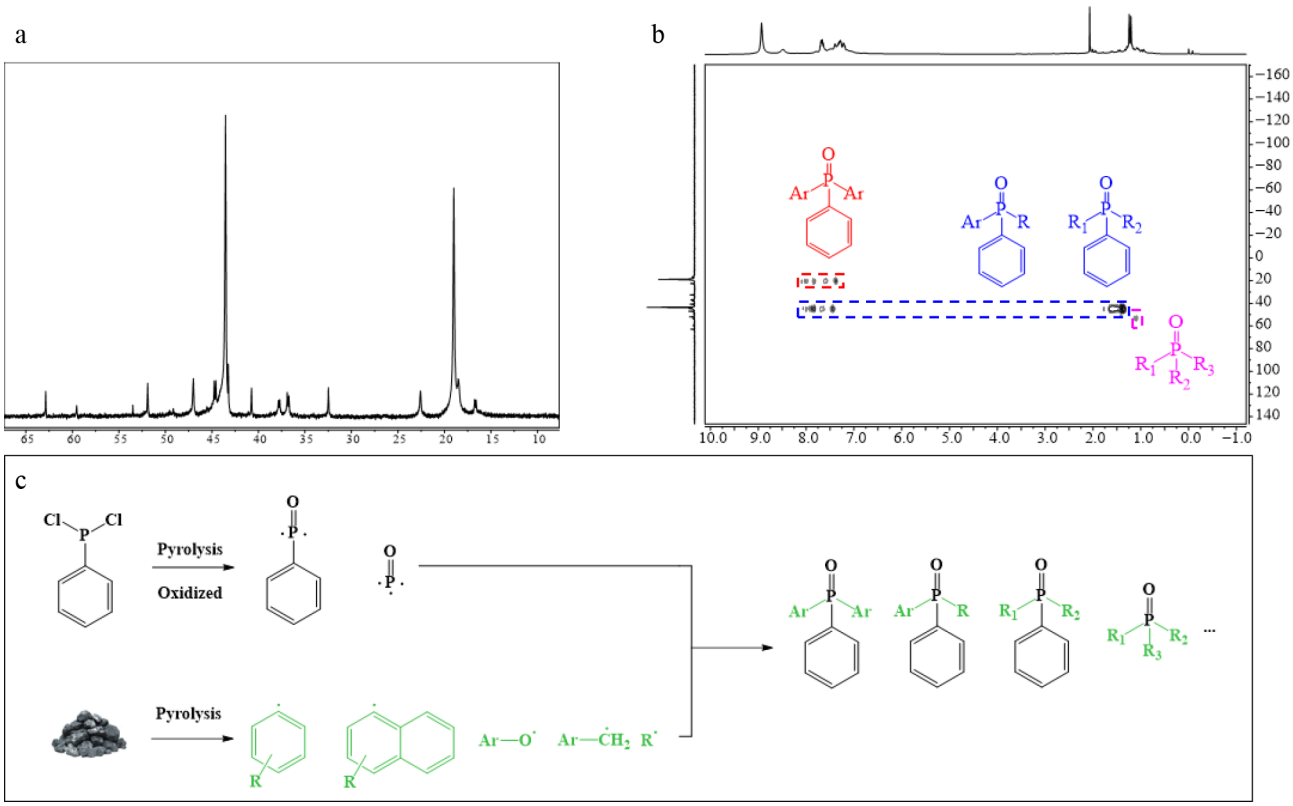

Fig. 7 NMR spectra and mechanism diagrams of the co-pyrolysis products of phenyldichlorophosphine and oil-rich coal. (a) ^{31}P NMR spectrum; (b) ^{1}H-^{31}P HMBC NMR spectrum; (c) mechanism diagram.

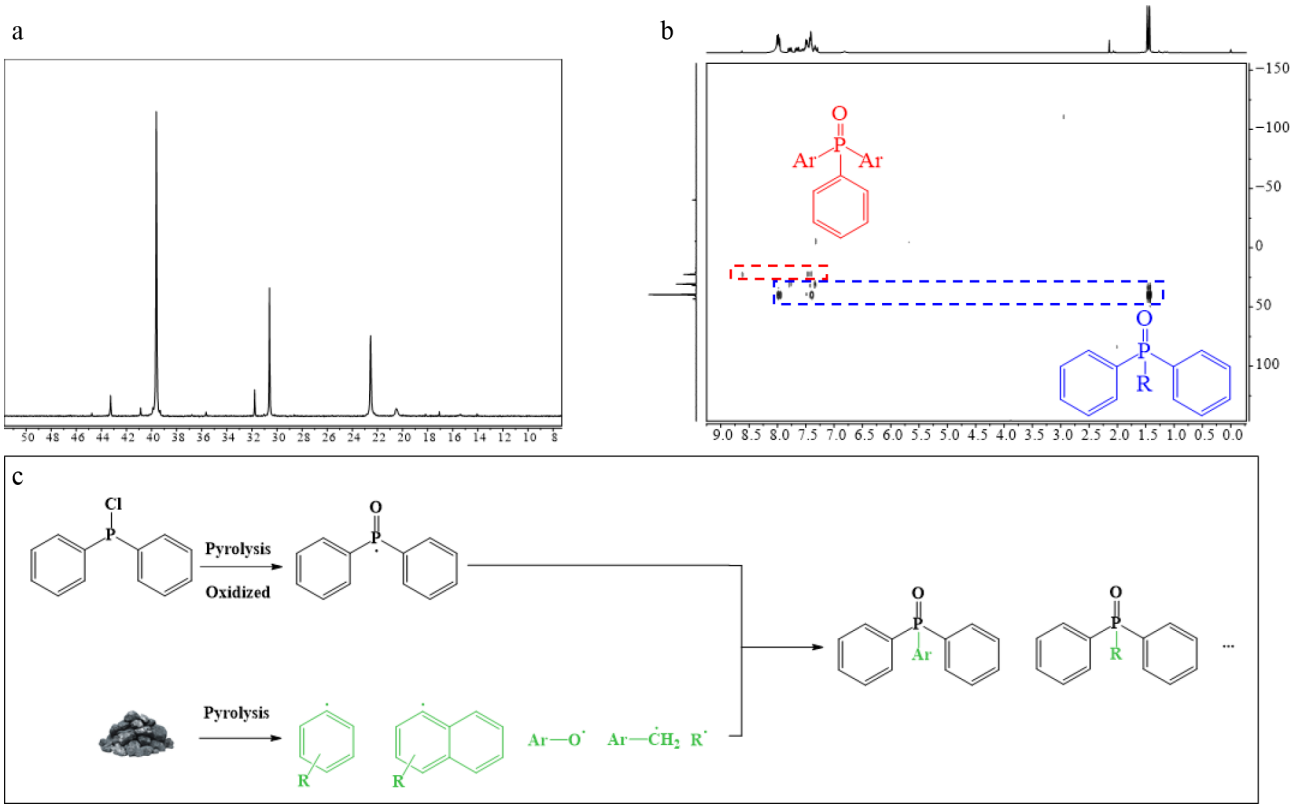

Fig. 8 NMR spectra and mechanism diagrams of the co-pyrolysis products of chlorinated diphenylphosphine and oil-rich coal. (a) ^{31}P NMR spectrum; (b) ^{1}H-^{31}P HMBC NMR spectrum; (c) mechanism diagram.

Conclusions

This study successfully prepared organophosphorus-rich tar through co-pyrolysis of oil-rich coal with phosphorus-containing compounds, and analyzed the structural characteristics of the products using various phosphorus compounds. Initially, inorganic phosphorus compounds were employed. Due to the high symmetry of phosphate tetrahedral units forming a delocalized π-system, phosphoric acid preferentially generated monophenyl phosphate. Phosphorus trihalides, characterized by low boiling points and high reactivity, tended to form phosphate derivatives. Phosphorus oxychloride was ultimately selected as the most effective reagent. ICP-OES analysis confirmed that the phosphorus content in the coal tar increased by more than 500-fold after introducing phosphorus compounds. However, due to the high boiling points of certain phosphorus compounds, only a portion of the low-boiling-point compounds could be detected via GC-MS. Consequently, GC-FPD was employed and identified 22 distinct phosphorus-containing compounds. NMR analysis revealed various phenyl-alkyl substituted phosphine oxides, phosphates, and partial phenyl-alkyl phosphines. Further structural confirmation was achieved using infrared spectroscopy. Leveraging the precision of NMR techniques, organic phosphorus compounds derived from the pyrolysis of oil-rich coal were also examined based on ^{31}P NMR and ^{1}H-^{31}P HMBC NMR spectra. The primary products from dimethyl phenylphosphonate were aryl-alkyl substituted phosphonates, while triphenyl phosphite pyrolysis yielded predominantly unsubstituted phosphonates. In contrast, alkyl-aryl substituted phosphorus compounds produced a wider variety of products, mainly comprising aryl phosphonates, hydrocarbon phosphonates, and aryl-alkyl substituted phosphonates. Future work will involve co-pyrolysis of a coal model compounds with isotopically labeled phosphorus compounds to elucidate radical reaction pathways, clarify the formation mechanisms of phosphine compounds, and provide a theoretical foundation for the high-value utilization of coal tar.

Author contributions

The authors confirm their contributions to the paper as follows: conceived the project and designed the research: Chen F, Luo Z; performed NMR experiment: Chen P, Su B, Li G; provided co-pyrolysis of rich oil coal: Wang N, Tian H, Zhou A; provided GC-MS analysis: Shi G, Zhang Y, Zhou A; carried out statistical analyses and structural analysis: Han X, Su B; wrote and revised the manuscript: Chen P, Wang Q. All authors reviewed the results and approved the final version of the manuscript.

Data availability

All the data generated or analyzed in this study are included in the published articles. The remaining data can be provided upon request.

Acknowledgments

This research was funded by the National Natural Science Fundamental Project (No. U24A20552, 32202164) for the financial support.

Conflict of interest

The authors declare that they have no conflict of interest.

Dates

Received 23 December 2025; Revised 2 February 2026; Accepted 16 March 2026; Published online 24 June 2026

References

[1] Wang S, Shi Q, Wang S, Shen Y, Sun Q, et al. 2021. Resource property and exploitation concepts with green and low-carbon of tar-rich coal as coal-based oil and gas. *Journal of China Coal Society* 46:1365−1377 (in Chinese)

[2] Zhao C, Ge L, Mai L, Li X, Chen S, et al. 2023. Review on coal-based activated carbon: preparation, modification, application, regeneration, and perspectives. *Energy & Fuels* 37:11622−11642

[3] Wang C, Zeng K, Sheng C, Zhang Q, Lu Y, et al. 2025. Design of a heat storage integrated fluidized bed reactor for solar-driven gasification of low-rank coal. *Fuel* 396:135354

[4] Wang K, Guo L, Zhai X, Deng J, Li Y. 2024. Hydrogen abstraction reaction mechanism of oil-rich coal spontaneous combustion. *Fuel* 367:131538

[5] Yang F, Gao K, Yu Z, Ma L, Cao H, et al. 2023. Thermodynamic analysis of *in situ* underground pyrolysis of tar-rich coal: primary reactions. *ACS Omega* 8:18915−18929

[6] Ma ZH, Li WL, Hu LY, Li L, Dong XQ, et al. 2025. Molecular recognition combined with sequential extraction of aromatics from high-temperature coal tar pitch for separating chemicals: a comprehensive study of experiment and quantum chemistry. *Renewable Energy* 241:122329

[7] Ge Y, Yu J, Lin J, Wang S, Luo K, et al. 2024. Multiphase flow and reactor optimization of a 1MWth pilot-scale circulating fluidized bed for coal staged conversion. *Chemical Engineering Journal* 484:149524

[8] Deng J, Lang W, Ouyang J, Li Z, Yuan S. 2024. Catalytic upgrading of coal tar to produce value-added chemicals and fuels: a review on processes, catalytic mechanisms and catalysts. *Chemical Engineering Journal* 500:157420

[9] Zhang M, Zang X. 2023. Application of principal-component analysis to the interpretation of coal tar physico-chemical properties. *Fuel* 338:127304

[10] Lv Q, Ma Y, Yao Q, Sun M. 2025. A Review on the extraction of phenols from coal tar: composition distribution and analysis, methods and mechanism, process and industrialization prospect. *Energy & Fuels* 39:1479−1506

[11] Chang QL, He GF, Chen MB, Sun HY, Liu YW, et al. 2023. Research progress in extraction chemicals from coal tar by high-value utilization technology. *Coal Quality Technology* 38:10−20 (in Chinese)

[12] Liu Y, Lin J, You Y, Zhong S, Zhang B, et al. 2025. Potassium ferrate catalyzed microwave pyrolysis: efficiently improving sludge bio-oil quality and heavy metals immobilization. *Journal of Environmental Chemical Engineering* 13:118733

[13] Zhang L, Gao J, Hou R, Fan X, Liang P. 2025. Role of lignite and derived semicoke in nitrogen fixation during co-pyrolysis of protein-rich biomass: physical or chemical adsorbent? *Chemical Engineering Journal* 521:166275

[14] Gai D, Shao D, An F, Zhong Z, Wang, X, et al. 2025. Targeted migration mechanisms of nitrogen-containing pollutants during chemical looping co-gasification of coal and microalgae. *Journal of Hazardous Materials* 487:137237

[15] Zou Z, Chen Y, Zheng J, Zhang X, He H. 2021. Co-combustion performance analysis of a Fujian anthracite with *Cunninghamia lanceolate* and Mycorrhizal plants. *Progress in Reaction Kinetics and Mechanism* 46:14686783211010966

[16] Wang H, Liu W, Xu S, Jiang H, Wang H, et al. 2025. Regulation of Ni single-atom/nanoparticle cooperative catalytic systems by P heteroatom asymmetric coordination for efficient electrocatalytic CO_2 reduction. *Small* 21:2504251

[17] Zhang Y, Yang J, Yu P, Ruan R, Dai L, et al. 2025. Catalytic co-pyrolysis of cotton stalks and ground film plastic using fishbone-based metal catalysts: enhanced production of olefins and aromatics. *Chemical Engineering Journal* 521:166274

[18] Feng J, Xu B. 2014. Reaction mechanisms for the heterogeneous hydrogenolysis of biomass-derived glycerol to propanediols. *Progress in Reaction Kinetics and Mechanism* 39:1−15

[19] Nejadmoghadam E, Achour A, Öhrman O, Salam MA, Creaser D, et al. 2024. Stabilization of fresh and aged simulated pyrolysis oil through mild hydrotreatment using noble metal catalysts. *Energy Conversion and Management* 313:118570

[20] He L, Yao Q, Wang W, Zhang S, Wang Y, et al. 2025. Mechanism of coal pyrolysis to produce aromatics and phenols under H_2 atmosphere: multi-step pyrolysis by Py-GCMS and DFT calculations. *Fuel* 393:134130

[21] Kang H, Xu Q, Cao Z, Lu X, Shi J, et al. 2025. A comparative study on evolution characteristics of organic functional groups and gases during low-rank coal pyrolysis in N_2 and H_2 atmospheres. *International Journal of Hydrogen Energy* 114:106−119

[22] Kang H, Xu Q, Cao Z, Chen B, Wei W, et al. 2025. Effect of coal addition on reduction behavior of hematite in a H_2 atmosphere. *Powder Technology* 466:121503

[23] Zheng S, Blaschek L, Pottier D, Dijkhof LRH, Özmen B, et al. 2025. Pupylation-based proximity labeling unravels a comprehensive protein and phosphoprotein interactome of the Arabidopsis TOR complex. *Advanced Science* 12:2414496

[24] Xie L, Tian H, Wang Y, Bi Y, Chen B. 2025. Eco-friendly and additive-free synthesis of C—P bonds: synergistic catalysis by a polyoxovanadate-based Cu–organic framework using molecular oxygen. *Advanced Synthesis & Catalysis* 367:e70206

[25] Fan Y, Qi R, Dong S, Zhang J, Shi S, et al. 2025. Exposure assessment for air-to-skin uptake of traditional and emerging organophosphate flame retardants. *Environment International* 2025:109728

[26] Hao C, Qiu Z, Yang Z, Hu G, Chang F, et al. 2025. Highly efficient photo-assisted degradation of waste plasticizers over atomically dispersed cobalt sites. *Small* 21:e06342

[27] Wang G, Du X, Nie Z, You H, Yin Q. 2025. Ru-catalyzed asymmetric reductive amination of benzyl ketones: asymmetric control enabled by synergistic interaction of both chiral bisphosphine and chiral amino-acid ligands. *Chinese Journal of Chemistry* 43:3199−3204

[28] Zhao SY, Huang YY, Deng SH, Guan ZP, Dong ZB. 2024. Photocatalytic C–P bond formation based on the reaction of carbon-centered radicals with phosphides. *Organic Chemistry Frontiers* 11:4882−4894

[29] Zhu Y, Wu L, Liu H, Yang W, Li H, et al. 2025. Catalytic pyrolysis of duckweed with phosphoric acid: products yield and composition. *Renewable Energy* 240:122287

[30] Chen Y, Yu Z, Jiang Z, Tan JP, Wu JH, et al. 2021. Asymmetric construction of tertiary/secondary carbon–phosphorus bonds via bifunctional phosphonium salt catalyzed 1, 6-addition. *ACS Catalysis* 11:14168−14180

[31] Fu X, Niu X, Zhang D, Li L, Ye X, et al. 2024. Insights into novel phosphorus-doped biochar for tetracycline removal: non-radical oxidation and adsorption. *Journal of Environmental Chemical Engineering* 12:114224

[32] Chen P, Li G, Shao J, Bai B, Hu J, et al. 2025. Preparation of nitrogen-rich tar by co-pyrolysis and analysis of nitrogen-containing compounds in pyrolysis products. *Applied Sciences* 15:6284

[33] Yi Y, Wang P, Fan G, Wang Z, Chen S, et al. 2020. Hierarchically porous carbon microsphere doped with phosphorus as a high conductive electrocatalyst for oxidase-like sensors and supercapacitors. *ACS Sustainable Chemistry & Engineering* 8:9937−9946

[34] Ma ZH, Li S, Dong XQ, Li M, Liu GH, et al. 2023. Recent advances in characterization technology for value-added utilization of coal tars. *Fuel* 334:126637

[35] Xu B, Wang C, Zhu X, Zhu L, Han G, et al. 2025. Comprehensive analysis of metabolic changes in mice exposed to corilagin based on GC-MS analysis. *Drug Design, Development and Therapy* 19:389−404

[36] EL-Saeid MH, Hassanin AS, Bazeyad AY, Al-Otaibi MT. 2021. Rapid analytical method for the determination of 220 pesticide with their isomers by GCMS-TIC. *Saudi Journal of Biological Sciences* 28:4173−4182

[37] Zhang S, Liu X, Qin J, Yang M, Zhao H, et al. 2017. Rapid gas chromatography with flame photometric detection of multiple organophosphorus pesticides in *Salvia miltiorrhizae* after ultrasonication assisted one-step extraction. *Journal of Chromatography B* 1068:233–238

[38] Wiktorko M, Kot P, Puchała A, Bryczek-Wróbel P, Rzadkowska KI, et al. 2025. Ultra-sensitive analysis of organophosphorus compounds by comparative GC-FPD and GC-ICP-MS: implications for chemical warfare agent detection. *Molecules* 30:4086

[39] Bhinderwala F, Vu T, Smith TG, Kosacki J, Marshall DD, et al. 2022. Leveraging the HMBC to facilitate metabolite identification. *Analytical Chemistry* 94:16308–16318

[40] Ma SP, Wang C, Chen AZ, Zhang XL, Wang DP, et al. 2025. Glycerophospholipids analysis using conventional ^{1}H-^{31}P HMBC and its application in revealing the characteristics of 18 seaweeds. *Journal of Agricultural and Food Chemistry* 73:10654–10664

[41] Choinopoulos I, Papageorgiou I, Coco S, Simandiras E, Koinis S. 2012. Modification of Wilkinson's catalyst with triphenyl phosphite: Synthesis, structure, ^{31}P NMR and DFT study of trans-[RhCl(P(OPh)$_3$)(PPh$_3$)$_2$]. *Polyhedron* 45:255–261